ROCO318 - Mobile and Humanoid Robots
Report - Sensors

Emily-Jane Rolley-Parnell[1], Alfred Wilmot[1]

I. Introduction

This section of the report includes the testing and implementation of a Phidget Spatial 3/3/3 1044 IMU[1]. There are 4 subsections: subsection II describes the functionality of the sensor and how each component works, subsection III describes the possible applications of an IMU in general, subsection IV collates the experimental data we have collected to compare the realistic limits with those provided by the datasheet, and finally subsection V, contains the conclusion for Part 1 of the report.

II. Functionality

This subsection will describe in detail the principle components of an IMU, in particular the *PhidgetSpatial Precision 3/3/3 High Resolution*[2] on which we run our experiments.

An IMU, inertial measurement unit, measures a body's specific force. It detects linear acceleration using one or more accelerometers and rotational motion using one or more gyroscopes. An issue with the gyroscopes is that they have zero drift, which must be compensated for to be used in most applications. This can be done by including a magnetometer which uses the magnetic fields of the earth to eliminate this offset.

1) Accelerometer: The accelerometer measures the three linear accelerations of the body of the IMU. When the device is stationary, the acceleration, including acceleration due to gravity, would be of magnitude $\sqrt{a_x^2+a_y^2+a_z^2} = 9.81 m/s^2$ where $a_x(t)$, $a_y(t)$ and $a_z(t)$ can be used to find the momentary acceleration in each directional axis.

In order to correct for gravity you will need to determine the tilt angle and subtract $9.81 m/s^2$ in that axis. This means that if you want to measure dynamic acceleration, you must be sure that the range of readings available includes the ability to measure $9.81 m/s^s$ less than the minimum reading. Otherwise it may cause the accelerometer to reach its saturation value at a lower acceleration. Tilt angle can only be measured when the accelerometer is stationary. When in motion, the acceleration experienced by the accelerometer is a combination of the devices physical orientation, and the devices movement, and the tilt can therefore not be determined.

Integrals can be used to estimate velocity from a set of acceleration values. Likewise, if you integrate a set of velocity values, the result is an estimate of the position. This information is useful for any attempt at calculating a global position based on dead-reckoning.

2) Gyroscope: A MEMS, Microelectronical-Mechanical System, gyroscope is a device used for measuring orientation. A gyroscope contains small strips of metal that bend when the gyroscope moves. The angular velocity can be measured by monitoring the bending of the small strips. To give a usable value, the gyroscopes must be calibrated initially in a factory setting.

3) Magnetometer: There are two basic types of magnetometer measurement. Vector magnetometers measure the vector components of a magnetic field. Total field magnetometers or scalar magnetometers measure the magnitude of the vector magnetic field. Magnetometers used to study the Earth's magnetic field may express the vector components of the field in terms of declination (the angle between the horizontal component of the field vector and magnetic north) and the inclination (the angle between the field vector and the horizontal surface). Magnetometers are divided in to laboratory magnetometers and survey magnetometers. For use in the laboratory, the magnetometers are required to measure the magnetic properties of a material. Whereas survey magnetometers are further divided in to two, Scalar magnetometers to measure the total strength of a magnetic field but not its direction; or Vector magnetometers which measure the component of the magnetic field in a specific direction, relative to the device. The most common causes of error are interference with the compass component.

4) Components of PhidgetSpatial 3/3/3 1044: This IMU in particular contains an accelerometer, gyroscope and magnetometer, as well as a backup accelerometer and backup gyroscope. All of these are controlled by a microcontroller that can be interfaced with by USB.

III. Applications

IMUs are applied in many situations where orientation is required but accuracy is not crucial. The following are applications where IMUs have been used.

[3] is a paper in which the aim is to measure absolute orientation of an Ocean Bottom Seismometer, OBS, relative to magnetic north, with a PhidgetSpatial 3/3/3 1044 IMU. The seismometer (or geophone) is a detector that is placed in direct contact with the earth to convert very small motions of the earth into electrical signals, which are recorded digitally. OBS are designed to record the earth motion under oceans and lakes from man-made sources. These sensors are deployed to a depth of up to several kilometers, and on descent, undergo random rotations; therefore an IMU is

[1]University of Plymouth, Drake Circus, Plymouth, Devon PL4 8AA, United Kingdom. {emily-jane.rolley-parnell, alfred.wilmot}@students.plymouth.ac.uk

used to measure the angular displacement of the OBS and retrieve the absolute horizontal orientation.

[4] implemented a method of collecting more accurate orientation data from IMU and MARG (Magnetic, Angular Rate, and Gravity) devices, by applying gradient descent to the sensor values to extrapolate a more accurate and consistent reading. In the further work section of this paper, they describe that they will use this more accurate IMU data to generate a dead reckoning position. This is carried out in [5]. his paper describes a method for using accelerometer data combined with orientation estimates from the same modules to calculate position during walking and running. Relative position is calculated through double integration of drift corrected accelerometer data. The problem with this method is that the drift correction is not perfect and may produce erroneous data due to low accuracy and noisy data of the Micro Electro Mechanical System (MEMS) technology.

Our initial plan with this project was to create a method of tracking the position of an IMU using dead reckoning, with the purpose of applying it as a Cartesian controller for the end effector of a robotic arm. After reading the related works, we decided that the conceivable outcome would not be a worthy result given the time limit. Instead we decided to apply the time better to completing in depth experiments to measure the performance characteristics of a small sample of IMUs.

IV. Experimental Data

The measurement devices themselves have a fixed precision that can be found on page 16 of the manual [1], while these characteristics are approximately correct, there will be variance between devices, as we demonstrate below. The testing regime we developed is as follows: First in Section IV-.1, we test the limits of the IMU individually, then comparing these to the data sheets provided by Phidget. Second in Section IV-.4, we measure the noise of each IMU in various orientations. We measure the mean and standard deviation of noise for any one sensor and also quantify this using Allan Deviation. Third, we measure the quality of the calibration algorithm provided by Phidget by comparing magnetometer readings before and after. Fourth, we compare accelerometer readings against predicted value by moving the IMU down a ramp in orthogonal orientations at a fixed angle and calculate approximate acceleration algebraically. We also compare each of the variables in the data sheet with those that we measure across 10 IMU devices.

1) Physical Rig: In order to make these experiments as repeatable as possible, we designed and created a 3D printable chassis. This chassis is designed so that each IMU may be attached in various orientations, and kept stationary in these pre-determined orientations. It also allows that the orientation will be the same for every IMU tested. This chassis was designed for the particular experiment of Acceleration Validation in Section IV-.5. Its shape allows it to smoothly slide along the rod in this experiment with minimal jitter as well as minimal friction. Fig 1 contains a CAD design of the rig as well as a photo of the rig with affixed weighted bolts.

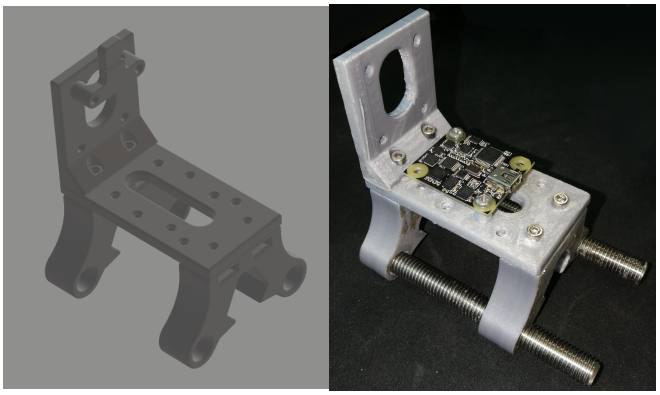

Fig. 1: Image containing both the STL file for the rig design and a photo with the IMU fixed to the rig.

2) Magnetometer Calibration: To collect the most accurate data from the IMUs we will test on, In order to complete one calibration cycle for one IMU, we must first find the Magnetic Field Strength at the location of testing. We used a website that, given latitude and longitude, provides this Magnetic Field Strength [6]. For the Location of Plymouth, England with the latitude 50 22' 17.5" N and Longitude 4 8' 35" W, The Magnetic Field Strength for this location is 48351.2 nT or 0.48 Gauss. We then use the included CompassCalibrator.exe to find the offset, gain, T, and measured magnetic field. The completed dataset of all the calibration data for all 10 IMUs across approximately 1000 samples are found in Table I. This gives a graphical representation of how the calibration output parameters shift and transform the error-filled sampled data into a close approximation of a sphere. This can be used to visually validate the accuracy of the calibration. An example of this is shown in Fig 2.

In Fig 2, there is a clear difference between the sample data and the calibrated data. As the data was collected while mounted on to the 3D printed rig, the calibration should counteract any interference caused by "Hard Iron" or "Soft Iron" interference. In this case, it may be caused by the mounting screws and the metal rods that are part of the design. However because it would be a challenge to complete the calibration process while mounted on

3) Limits Testing: When testing the saturation limits of the linear and angular acceleration sensors of the IMUs being tested, the results reflected the limits specified in the datasheet.max linear acceleration 8g. Max angular acceleration 2000 deg/s.

4) Measuring Noise: In this section we explore the noise measured across a frequency spectrum. We do this by sampling the x, y, and z values for acceleration from the IMU accelerometer. The range of frequencies is from a minimum of *4ms* to *964ms* in *40ms* steps. From each of the samples taken from IMU 302056 we can observe that the standard deviation is significantly higher when the sampling time period is 44ms, when the frequency is 1/44ms = 22.7Hz.

Serial #	magField	Offset(0)	Offset(1)	Offset(2)	Gain(0)	Gain(1)	Gain(2)	T(0)	T(1)	T(2)	T(3)	T(4)	T(5)
302056	0.33263	0.00458	0.13092	0.17761	2.98445	2.98384	3.05064	-0.02632	-0.00963	-0.02582	0.01774	-0.00947	0.01807
302030	0.34038	-0.00925	0.16973	0.01454	2.84040	2.78162	3.19164	0.01039	-0.02240	0.00953	0.03287	-0.02491	0.03816
415639	0.33680	-0.12072	0.01082	0.27409	2.78589	2.88528	3.23618	-0.03603	-0.04122	-0.03632	0.03311	-0.04641	0.03742
414955	0.33208	-0.12917	0.01162	-0.01674	2.85633	2.87211	3.30567	-0.03216	-0.02322	-0.03204	0.02141	-0.02647	0.02450
302099	0.35763	0.01054	0.15044	-0.28300	2.63704	2.62570	3.12588	-0.00137	-0.03954	-0.00136	0.05165	-0.04540	0.06100
354036	0.35683	0.07391	0.12645	0.03986	2.71077	2.57574	3.12084	-0.01494	-0.10392	-0.01378	0.01435	-0.11751	0.01826
353944	0.35868	0.08644	0.10253	0.10556	2.55849	2.67852	3.12706	-0.12412	-0.17543	-0.14070	-0.12041	0.13788	-0.01069
302047	0.35762	0.01827	0.16790	-0.00536	2.67138	2.72759	2.98991	-0.03220	-0.03450	-0.03194	0.04328	-0.03726	0.04785
417738	0.33749	-0.12424	0.00791	-0.04667	2.80900	2.87341	3.20674	-0.00118	-0.03973	-0.00061	-0.05388	-0.04408	-0.06087
302088	0.34276	-0.00335	0.15939	-0.07763	2.81062	2.70176	3.24011	-0.06659	-0.08950	-0.05962	0.05574	-0.10060	0.06719

TABLE I: Table to show the key calibration data points for each IMU.

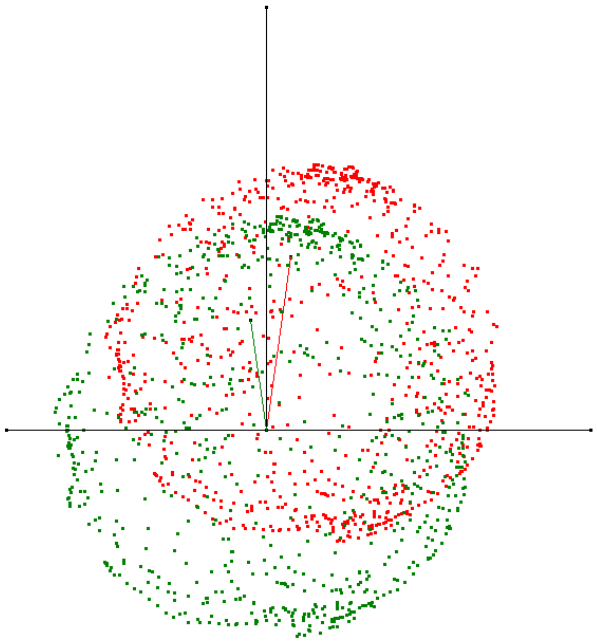

Fig. 2: Graphical visualisation of comparison between sampled data from the magnetometer (the red points on the graph) and the calibrated data from the magnetometer (green data points).

5) Acceleration Validation: In order to validate the the accuracy of the accelerometer readings, a test was designed whereby the IMU is mounted into a chassis and made to slide down a rail in a controlled, repeatable manner, in such a way that the IMU is able to move linearly along only one of it's axes. Isolating motion to a single axis in this manner enables for the modelling of acceleration experienced by the IMU along this axis to be done using simple geometry. The experimental setup can be seen in Figs 6 and 7. The same python software developed for the static-tests was also used in the dynamic experiment for rapidly gathering and visualizing the data, at any of the sampling periods allowed for by the IMU SDK (min 4ms, max 1000ms, in steps of 4ms). For the dynamic experiment, three IMU's were put under test. Only the IMU_z axis was tested for all three. Each IMU was tested three times at 4ms sampling rate, and three times at 12ms sampling rate. Fig 4 shows an example of the code in use.

The length of the rail is 1.6 meters, and the angle between the ground α and the rod was 59.036 degrees. Acceleration vectors due to friction from physical contact between the chassis and the rail and air resistance are negligible. Any friction present during the tests, results of which are shown in the IMU_z graphs in Fig 9, is apparent as an offset from pure free-fall (0 acceleration) during the dynamic stage of the test. IV-.5. With this in mind, the acceleration in the X and Y axes should be constant. In order to validate the acceleration measured in a dynamic setting, we compare the measured values of the X and Y axes with the calculated values. To calculate the acceleration when stationary based on the settings, we use trigonometry.

$$a_z = g \times sin\theta$$

$$a_z = -9.81 \times sin59.036 = -8.411 m/s^2$$

Therefore the acceleration along the IMU_z axis, a_z is $-8.411 m/s^2$ or $-0.857g$ where g is $9.81 m/s^2$. This is validated by the reading along the IMU_z axis in each of the test drops in Fig 9, and seeing that the value is approximately $-0.85 m/s$, we approximate that the Z axis accelerometer is reading correctly when stationary.

The acceleration along the Y Axis may be calculated as follows:

$$a_y = -g \times cos\theta$$

$$a_y = -9.81 \times cos59.036 = -5.047 m/s^2$$

The acceleration along the Y axis, a_y is then $-5.047 m/s^2$ or $-0.514g$. The accelerometer reading during the experiment gives approximately $0.514g$ due to the orientation of the accelerometer axes internally.

Due to the physical filtering provided by the rail, we can estimate that the acceleration along the X axis will be 0 as there is no physical movement along this axis. In actuality there is a small amount of movement due to the non-perfect fitting of the rig to the rod. This prediction matches our measured readings.

From the sample, we then take the absolute difference between the estimated acceleration and the measured acceleration for each IMU on each X and Y axis. We used 3 IMUs to test this, IMU 302030, 302047 and 353944. Respectively, the drop experiments had an average time length of $753.3 ms$ with a standard deviation of $16.1 ms$. We deemed this to be

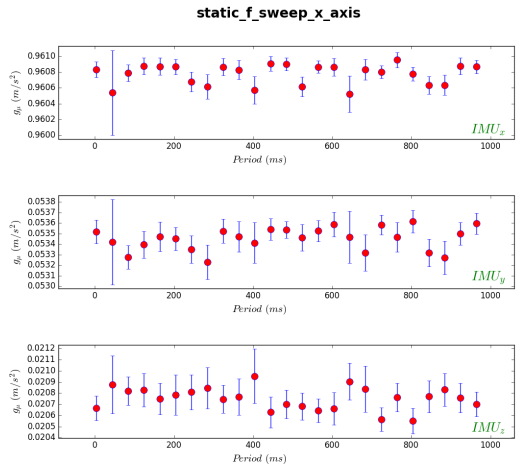

(a) X Axis

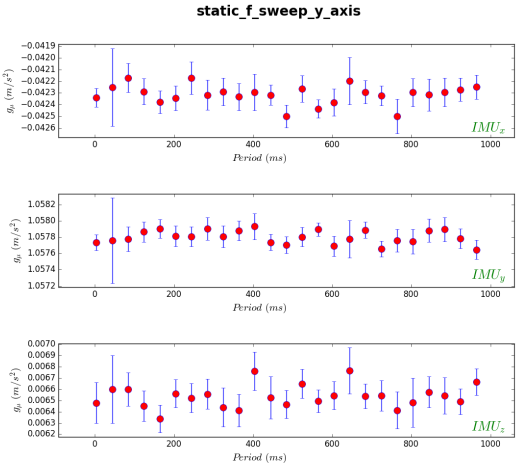

(b) Y Axis

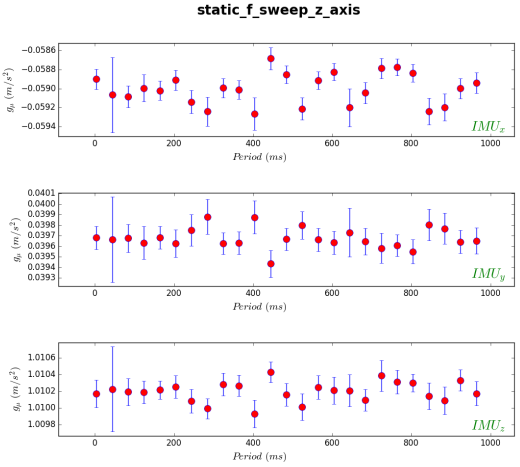

(c) Z Axis

Fig. 3: The graphs to show the standard deviation of measurements when the IMU is stationary at different frequencies. Each section is an experiment across frequencies while the IMU is positioned in different orientations. The subheading for each graph corresponds to the axis that is perpendicular to the force of gravity.

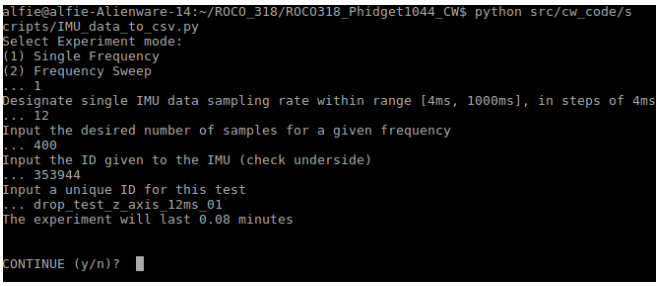

Fig. 4: Terminal interface being used to set-up an experiment at a sampling period of 12ms.

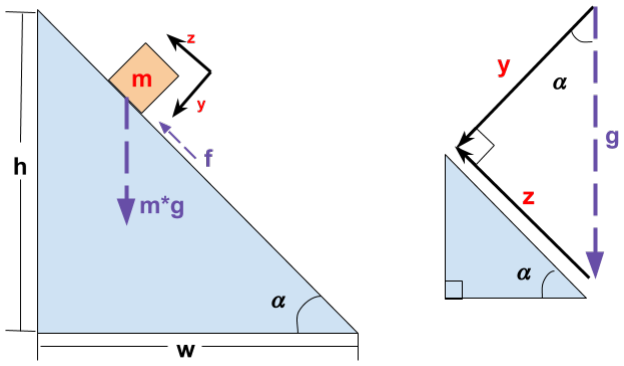

Fig. 5: Force diagram to display the forces acting on the rig.

a reasonable standard deviation as the initial friction before release varies depending on how the rig is held.

To measure the error, we calculated the difference between each data sample and the predicted value for the dynamic period. For each X axis accelerometer, the average error came to $0.121g$, $0.104g$, and $0.073g$ respectively. The variance calculated for the X axis was given to be 0.58×10^{-3}.

We also compare along the Y axis, again calculating the difference between the sample value and the predicted acceleration to be measured along that axis. For each Y axis accelerometer, the error came to $0.082g$, $0.083g$, and $0.084g$ respectively. Therefore the variance between devices is 1.72×10^{-3}.

We can observe that the average error measured in the X axis is less than in the Y axis. We believe this to be because the rig design allowed more movement vertically rather than horizontally. To improve the reliability of these tests, we would redesign the rig to reduce the clearance in the Y axis to match the clearance in the X axis. We can then state that the variance in noise across different IMUs along the X axis during a dynamic period is small enough to be negligible in this medium scale application.

V. Conclusion

From our experiments, we conclude that the Phidget Spatial 3/3/3 1044 accelerometers are manufactured to a standard that the variance between devices is negligible. With more time, we would have liked to observe the Allan

Fig. 6: Chassis mates into rail guide, thereby constraining motion to a single IMU axis.

Fig. 7: Chassis moves linearly along rail until reaching a dead-stop.

Variance of the noise measured for each IMU. As Allan Deviation gathers data about the noise of the specific sensor in use, it is helpful to remove noise in future experiments. Allan Deviation is performed on data sets of various sizes to find the smallest number of points required to minimize the variance in the group average. We would also have liked to attempt the drop test in IV-.5 along multiple axes so that we may cross validate the error measured as well as being able to validate the accelerometer in the Z axis.

References

[1] *Product Manual 1044 - PhidgetSpatial 3/3/3*, Phidgets, July 2012.

[2] "Phidget website," https://www.phidgets.com/?&prodid=32, accessed: 05-01-2019.

[3] A. DAlessando and G. D'Anna, "Retrieval of ocean bottom and downhole seismic sensors orientation using integrated mems gyroscope and direct rotation measurements," *Advances in Geosciences*, vol. 40, pp. 11–17, 12 2014.

[4] S. O. H. Madgwick, A. J. L. Harrison, and R. Vaidyanathan, "Estimation of imu and marg orientation using a gradient descent algorithm," in *2011 IEEE International Conference on Rehabilitation Robotics*, June 2011, pp. 1–7.

[5] X. Yun, E. R. Bachmann, H. Moore, and J. Calusdian, "Self-contained position tracking of human movement using small inertial/magnetic sensor modules," *Proceedings 2007 IEEE International Conference on Robotics and Automation*, pp. 2526–2533, 2007.

[6] "Magnetic declination," http://www.magnetic-declination.com/, accessed: 05-01-2019.

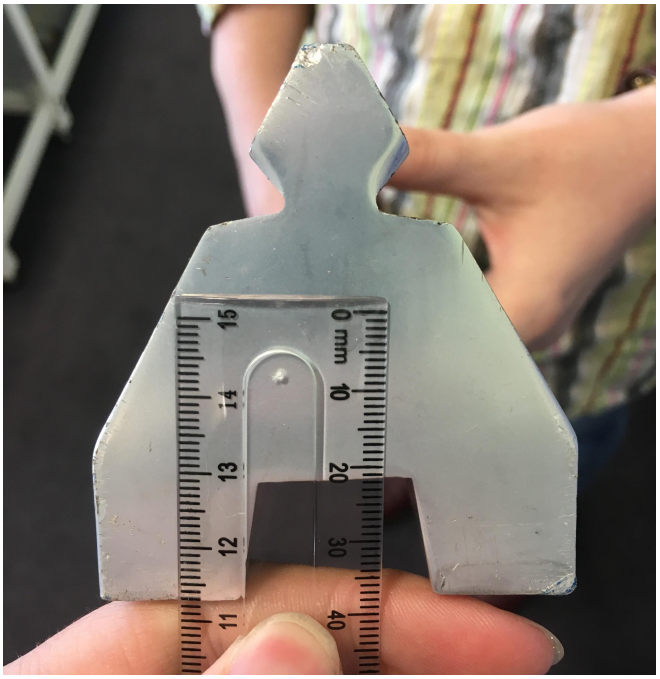

Fig. 8: Cross section of the rail used in the experiment.

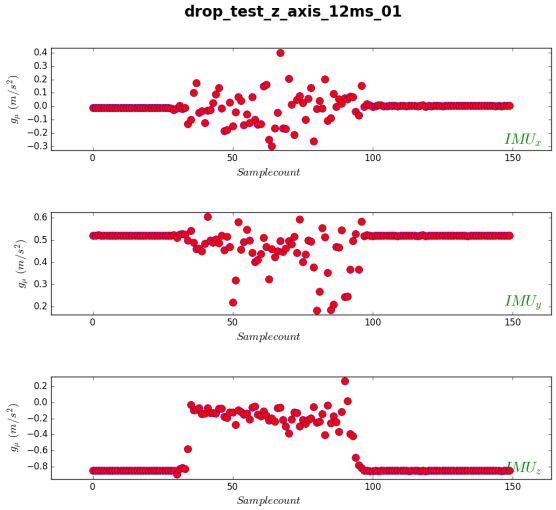

(a) IMU ID:353944

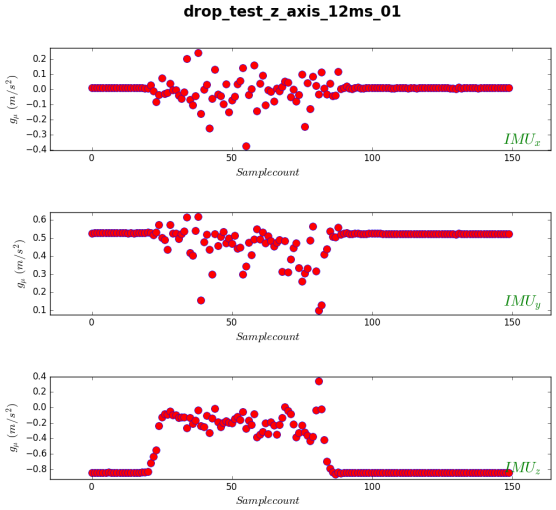

(b) IMU ID:302030

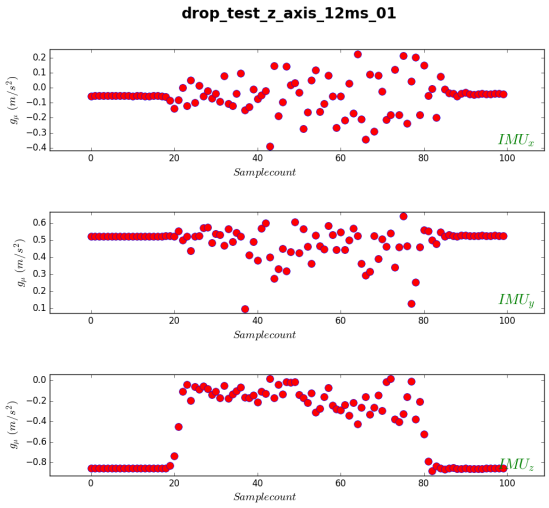

(c) IMU ID:302047

Fig. 9: The graphs for 3 different IMUs to show the variance in reading for the same motion, at a sampling time period of 12ms.